Available online at www.sciencedirect.com
SCIENCE DIRECT
Journal of Non-Crystalline Solids 352 (2006) 2601–2617
JOURNAL OF NON-CRYSTALLINE SOLIDS
www.elsevier.com/locate/jnoncrysol

Self-trapped holes in pure-silica glass: A history of their discovery and characterization and an example of their critical significance to industry

David L. Griscom *

Materials Science & Engineering, University of Arizona, Tucson, AZ, 85721-0012, USA
impactGlass Research International, 3839 E Grant Rd #131, Tucson, AZ 85712-2559, USA

Available online 24 May 2006

Abstract

It has long been assumed that hole self-trapping should take place in amorphous silicon dioxide (a-SiO_2). However, no spectroscopic evidence for this was claimed before 1989, when the author used electron spin resonance (ESR) to identify self-trapped holes (STHs) in bulk samples of low-OH pure fused silica X irradiated $\leqslant$100 K, and Chernov et al. reported a low-temperature infrared absorption near 1600 nm in irradiated pure-silica-core fibers, which they ascribed to STHs. Based on g values and ^{29}Si and ^{17}O hyperfine coupling constants measured by ESR, Griscom [D.L. Griscom, Phys. Rev. B 40 (1989) 4224; D.L. Griscom, J. Non-Cryst. Solids 149 (1992) 137] deduced the existence of two types of STHs: STH_1 (a hole trapped on a single bridging oxygen) and STH_2 (a hole delocalized over two equivalent bridging oxygens of the same SiO_4 tetrahedron). The validity of Griscom's models for STH_1 and STH_2 are supported by the ab initio calculations of Pacchioni and Basile [G. Pacchioni, A. Basile, Phys. Rev. B 60 (1999) 9990] and Gabriel [M.A. Gabriel, PhD dissertation, Department of Chemistry, University of Washington, Seattle, WA, in preparation]. In 1984, Nagasawa et al. reported that low-OH-pure-silica-core optical fibers γ irradiated at $\sim$300 K exhibit metastable optical absorption bands at 660 and 760 nm. Griscom [D.L. Griscom, J. Non-Cryst. Solids 349 (2004) 139] recorded these same bands in low-OH-pure-silica-core fibers γ irradiated at 77 K, showing their isochronal annealing behaviors to correlate with his earlier ESR data for STHs in bulk silica and also with Harari et al.'s data [E. Harari, S. Wang, B.S.H. Royce, J. Appl. Phys. 46 (1975) 1310] for trapped positive charges in silica thin films following X irradiation at 77 K. Sasajima and Tanimura [Y. Sasajima, K. Tanimura, Phys. Rev. B 68 (2003) 014204] established direct correlations of an induced band at 574 nm with STH_2 by performing both ESR and a variety of optical measurements on three types of high-purity bulk silicas following pulsed electron irradiations at 77 K; however, these authors did not detect the 660 or 760 nm bands. Yamaguchi et al. [M. Yamaguchi, K. Saito, A.J. Ikushima, Phys. Rev. B 68 (2003) 153204] demonstrated that the yield of ESR-detected STHs photoinduced in bulk pure-silica samples at 77 K depends exponentially on fictive temperature (T_f). The present paper recounts the forgoing history in greater detail, while attempting to reconcile some seemingly disparate findings into a unified picture of STHs in silica. In the fall of 1998, a number of satellites in orbit were tumbling out of control due to failure of their HeNe ring-laser-gyro (RLG) attitude control systems. The author, acting in the capacity of pro-bono US government consultant, proposed the correct solution to this problem (replace Al-contaminated silica mirror coatings with high-purity ones). However, accelerated tests (short operation times at much-higher-than-normal laser powers) of the corrected devices failed to corroborate this fix. Thus, all further launches of satellites employing these RLGs remained grounded until the author was able to convince industry troubleshooters that (1) the accelerated test failures were due to the 660-nm STH band (which is induced even in the highest-purity silica coatings by 20-eV photons emitted by the laser plasma), (2) the strength of this band is initially proportional to ionizing dose rate (*inevitably giving false positives in accelerated tests*), and (3) this band eventually disappears after several months of irradiation, even at dose rates as low as 0.15 Gy/s. All of these insights derived from *curiosity-driven* components of the author's research.

* Tel.: +1 520 829 4601.
E-mail address: david_griscom@yahoo.com

0022-3093/$ - see front matter © 2006 Elsevier B.V. All rights reserved.
doi:10.1016/j.jnoncrysol.2006.03.033

PACS: 61.80.−x; 71.38.Ht; 76.30.Mi; 78.70.−g

Keywords: Band structure; Optical fibers; Radiation effects; Optical spectroscopy; Defects; Absorption; Silica; Electron spin resonance

1. Introduction

1.1. Self-trapped carriers in crystalline and glassy insulators

Color centers in insulating materials arise from trapping of (usually radiation-induced) free electrons or holes at sites of point defects in a crystal lattice [1] or glassy network [2,3]. Arguably the most fundamental color centers in any insulator are the 'self-trapped' carriers, i.e., electrons or holes which manage to trap at 'perfect' sites in the crystal lattice or glass network. In alkali halide crystals, mobile holes can become self-trapped by formation of small polarons [4], which involve local atomic relaxations surrounding a hole. Typically, self-trapped carriers are only stable at cryogenic temperatures. The most famous examples are the so-called V_K centers in alkali halides (e.g., [1,5]). V_K centers involve two halide ions X^- relaxing symmetrically towards each other so that the shared hole becomes localized in the σ antibonding orbital of the resulting X_2^- molecular ion. In the 1950s and 1960s, V_K centers were studied in immense detail by electron spin resonance (ESR) and optical methods (e.g., [1,5]).

In glasses, no site is truly 'perfect' in the same sense as sites in a crystal can be. Still, a silica glass can be said to be free of defects if it comprises an ideal continuous random network [6] of apex-connected SiO_4 tetrahedra and is free of impurities, broken bonds, vacancies, or abnormal coordination numbers. Thus, self-trapping of carriers by small polaron formation can be envisioned in such 'perfect' glasses. However, as first pointed out by Anderson [7], there is a second way by which electrical carriers can be trapped in amorphous materials that results from the vitreous randomness itself (and therefore may not *require* relaxations). Mott [8,9] termed these 'Anderson-localized' carriers and extended the notion to include carriers trapped above or below 'mobility edges' (see Fig. 1). Thus, self-trapped holes in amorphous semiconductors or insulators can be described as being trapped above mobility edges that transect exponentially decreasing band tails of normally filled states extending upward from the valence band into the band gap.

1.2. If there are self-trapped holes in SiO_2, where have they been hiding?

In principle the most fundamental defect in silicon dioxide should be the self-trapped hole (STH). However, a very careful attempt to find ESR spectroscopic evidence for STHs in a crystalline polymorph of SiO_2 (α-quartz) was unsuccessful, evidently because the activation energy for hole hopping was too small to confine a hole to a single lattice site long enough for measurement near 4 K [10]. But the existence of less-mobile STHs in *amorphous* (a-)SiO_2 has always seemed intuitively reasonable. Why then were not they found 'in the beginning', as were V_K centers in alkali halides in 1957 [5]? The main answer to this question is that, whereas single-crystal ESR experiments conducted

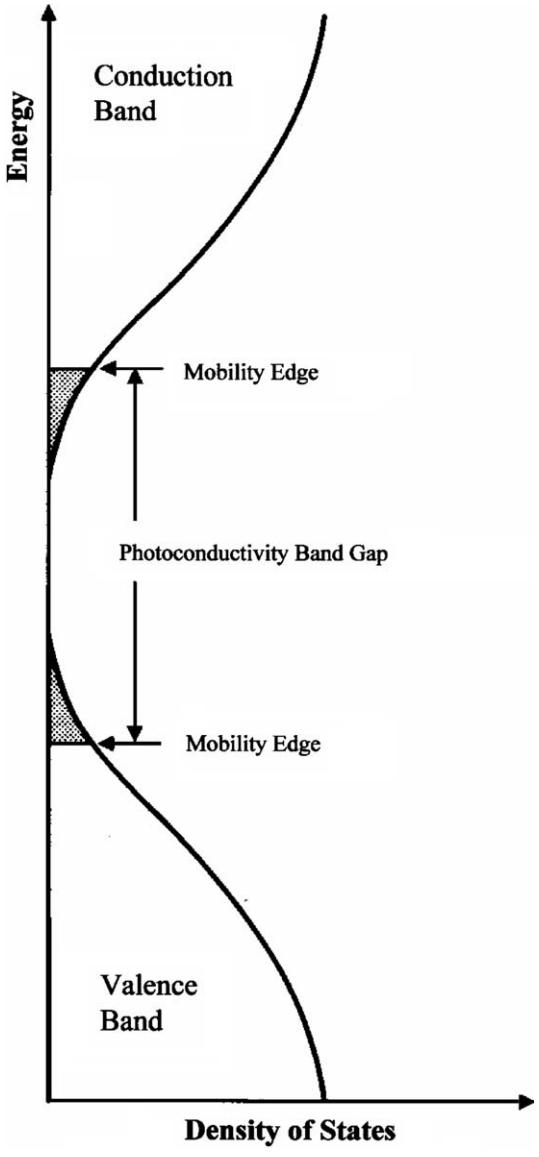

Fig. 1. Schematic diagram of the valence- and conduction-band densities of states for amorphous semiconductors and insulators. The optical band gap (depending on its definition) is usually smaller than the photoconductivity gap, which may be determined by mobility edges [8,9]. Radiation-induced holes (electrons) may trap above (below) the valence-band (conduction-band) mobility edge. (Adapted from [8].)

by skilled solid state physicists led quickly to unambiguous answers regarding color centers in crystals with angle-dependent ESR spectra (see, e.g., [1]), these same investigators were repelled by the ambiguities endemic to amorphous systems, which are devoid of the one feature that makes single-crystal ESR so powerful – crystal symmetries.

So the job of deciphering the glasses was left to a new generation of physicist/materials scientists, whose motivation, innovation, and risk-taking partially compensated for the missing (and now almost extinct) skills of the single-crystal ESR specialist. The second part of the answer lies in the fact that investigators found it quite difficult to separate and identify several overlapping 'oxygen hole center' spectra (first recognized by Bob Weeks [11]), all of which fell within the expected ESR spectral range for STHs. Given this combination of factors, it seems entirely possible that most concerned scientists became convinced that there were no more 'oxygen hole centers' to be found in a-SiO_2 after the eventual decomposition of Bob Weeks' 'oxygen hole centers' into components corresponding to the non-bridging-hole center (NBOHC) [12,13] and the peroxy radical (POR) [13,14] ca. 1979. However, the fallacy in this thinking was that, whereas the NBOHCs and PORs are stable defects that were usually studied after irradiation at room temperature, STHs are typically stable *only at cryogenic temperatures*.

As will be described below, it turns out that ESR spectra attributable to STHs in a-SiO_2 were published as early as 1971 [15], but they were not recognized as such until 1989 [16]. At that late date, several seemingly unrelated scientific story lines that I had been following suddenly converged – leading me to postulate the existence of STHs in a-SiO_2 as the unifying factor.

1.3. Story of the discovery of self-trapped holes in a-SiO_2

Fig. 2 presents a history of the discovery and characterization of STHs in a-SiO_2. It includes four separate timelines (horizontal gray streaks) representing the research activities of nine different research groups. Each large solid triangle indicates the date of a significant publication. In 1971, Arkadi Amosov and coworkers [15] published an ESR spectrum that, in '20–20' hindsight, is clearly attributable to the STHs. However, Arkadi's fused-natural-quartz sample contained significant impurities, leading him to ascribe its peculiar ESR signature to impurity-related defects. At that time, I tacitly accepted his reasoning. However, as I discussed in detail in 1992 [17], Arkadi's spectrum recorded immediately after irradiation at 77 K – and its thermally induced transformation into aluminum–oxygen hole centers upon warming – in retrospect match expectations for STHs induced in a-SiO_2 having Al and Ge impurities. But in 1981, when I finally observed the same ESR spectrum in a *high-purity* silica sample (first open triangle in Fig. 2), I had completely forgotten Arkadi's work of 10 years before. To me this seemed to be a 'new' spectrum – one that was quite different from those of the NBOHC and the POR. I knew it required a separate explanation, but it took me an additional seven years (second open triangle in Fig. 2) before I got the idea that this spectrum was

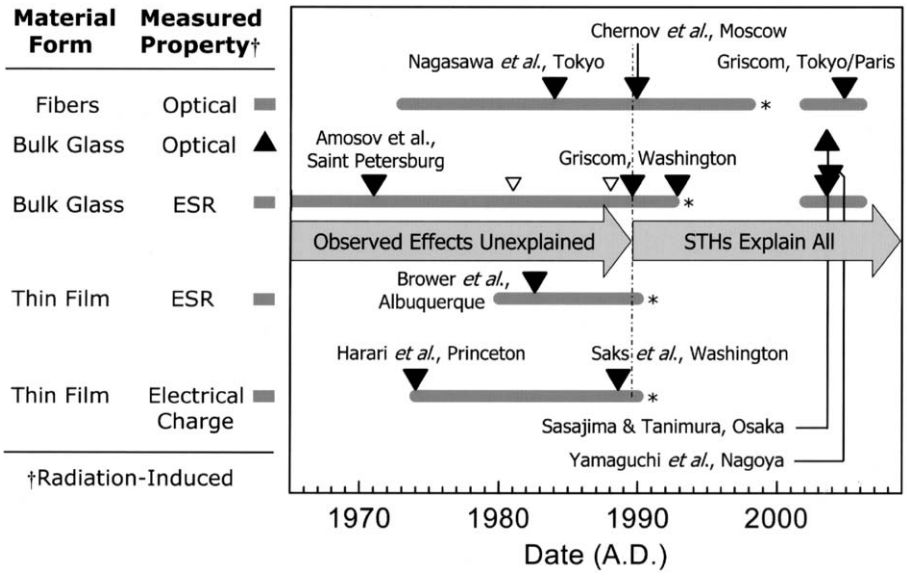

Fig. 2. A history of the discovery and characterization of self-trapped holes in amorphous SiO_2. Horizontal gray bars are timelines signifying quasi-continuous periods of experimental research in four of the five categories specified by the table at the left. By 'quasi-continuous' it is meant that the contributing researchers presumably had occasional mandates to do other things and/or they may have exercised their academic freedom to follow their scientific curiosity in other directions at various times during these intervals. Solid down triangles mark the dates of publications that (intentionally or not) led to significant clarifications of the natures of STHs in a-SiO_2. The single upward solid triangle pertains to optical measurements in bulk, rather than fiber, samples. Meanings of the open down triangles and asterisks are explained in the text. Note the 7- to 14-year intervals between landmark accomplishments even within periods of quasi-continuous activity. These data provide an indication of the 'time constant' of curiosity-driven basic research that it is allowed to proceed at its own pace.

possibly that of STHs. The catalyst for this epiphany lay in several invitations I had received from the nuclear and space radiation effects community to review the literature of interface states and radiation-induced defects in a-SiO_2 thin films thermally grown on silicon. Each of these reviews led to a publication [18–20].

While preparing my review lecture for the 1988 Electrochemical Society meeting in Atlanta, I was privileged to have available some pre-publication data acquired by Nelson Saks and coworkers [21,22] for oxide-trapped-charge and interface-state densities in metal-oxide-semiconductor field-effect transistors (MOSFETs) γ irradiated at 80 K and measured as functions of isochronal anneal temperature under different gate biases. Nelson's results immediately compelled me to abandon my earlier model for the *main* mechanism of interface-state creation, which I had proposed in [18] as

$$Si_3{\equiv}Si{-}H + H^{\cdot} \rightarrow Si_3{\equiv}Si^{\cdot} + H_2 \quad (1)$$

where the '$Si_3{\equiv}Si$' units belong to the silicon substrate at its interface with the thermal a-SiO_2 layer and $Si_3{\equiv}Si^{\cdot}$ is the so-called P_b (interface-state) center, which was first studied by ESR by Ed Poindexter and coworkers, e.g., [23]. In Eq. (1), each dot '$^{\cdot}$' signifies an unpaired electron. The atomic hydrogen ($H^{\cdot}$) on the left-hand side of this equation results from radiolysis of abundant OH groups in the oxide layer

$$\equiv Si{-}OH \rightarrow \equiv Si{-}O^{\cdot} + H^{\cdot} \quad (2)$$

In Eq. (2), '≡' represents bonds to three other oxygens in the oxide layer and the entity '≡Si–O$^{\cdot}$' is the NBOHC. The radiolytic $H^{\cdot}$ on the right-hand side of Eq. (2) is mobilized in a-SiO_2 at temperatures ~40–150 K [24–26].

Nelson Saks' data clearly showed that the reaction of Eq. (1) probably *does* occur in γ-irradiated MOSFETs near 100 K *as a bias-independent process*, but only in ~2% of the cases. The other 98% of the interface states evidently arise from positively charged entities originating in the oxide layer, which move to the interface at temperatures ~180–280 K under *non-negative* gate biases [19–22]. After assessing Nelson's quantitative data, I concluded [19] (i) that the positive oxide-trapped charge must *initially* be in the form of 'small polarons' (i.e., STHs) and (ii) that at temperatures in the range ~100–130 K these STHs should rapidly react with the thermally mobilized atomic hydrogen, thus creating protons H^+ (which at higher temperatures should transport toward the interface under neutral or positive electrostatic bias)

$$STH^+ + H^0 \rightarrow H^+ \quad (3)$$

Semiempirical and ab initio calculations of the reaction of Eq. (3) in SiO_2 have been reported by Art Edwards and coworkers [27]. The necessary hydrogen atoms were directly measured by ESR by Keith Brower and his coworkers [28] in a thermally grown oxide on silicon following γ irradiation at 4 K and were found to anneal out around 100 K. Significantly, Keith's data showed the atomic hydrogen in this a-SiO_2 film to have been outnumbered by 'oxygen hole centers' by a factor of ~3, thus assuring that virtually all H^0 would be consumed in the reaction of Eq. (3), leaving little available for the reaction of Eq. (1).

Not long afterwards, it occurred to me that the STHs that I had inferred to be the origin of the initially trapped positive charges in irradiated thermal-oxide films might be synonymous with the defects responsible for the 'new' hole-type ESR spectrum (actually already reported by Amosov et al. [15]) that I had observed ca. 1981 in a high-purity, low-OH synthetic silica (Suprasil W1) upon X irradiation at 77 K.

Accordingly, I submitted a letter-form report of my 'discovery' of the ESR spectrum of STHs that eventually achieved publication in 1989 [16] – just five months before publication of the work of Chernov et al. [29], who associated a γ-ray-induced optical band near 1800 nm with STHs. A crucial part of Chernov et al.'s argument was that the isochronal anneal characteristics of their 'low-temperature infrared absorption' (LTIRA) correlated well with the annealing of trapped *positive* charge measured by Harari et al. [30] in an a-SiO_2 thin film following X irradiation below 100 K. My isochronal-anneal data for the two principal ESR-determined STH variants STH_1 and STH_2 [16,17] (represented in Fig. 3 by up and down triangles, respectively) are also in good accord with Harari et al.'s data [30] for trapped oxide charge (solid circles in Fig. 3).

Finally, in my master paper on the subject [17] I was able to show that the composite STH_1-plus-STH_2 ESR

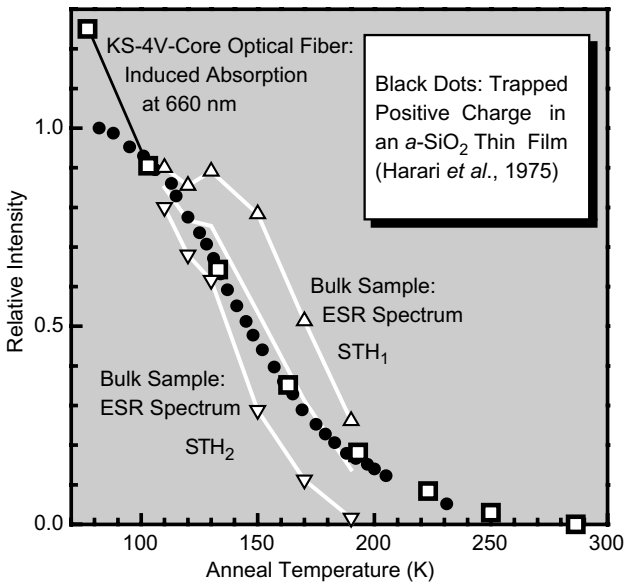

Fig. 3. Isochronal anneal data following X or γ irradiation at 77 K for the ESR manifestations of self-trapped holes in bulk a-SiO_2 (open triangles), trapped positive charges in an a-SiO_2 thin film (solid circles), and induced optical absorption measured at 660 nm in a low-OH, pure-silica-core optical fiber (open squares). The anneal times were 5 min in the case of the ESR data [16,17], unspecified in the case of the trapped-charge data [30], and ~13–16 min in the case of the fiber data [36]. Some data points are connected by straight-line segments as an aid to the eye. Middle white curve is an average of the STH_1 and STH_2 data. (From Ref. [36].)

spectrum of irradiated Suprasil W1 (see Section 2) is essentially identical with that of Keith Brower's 'oxygen hole centers'. Thus, although they did not mention it in their landmark paper [28], Brower, Lenahan, and Dressendorfer's ESR data qualitatively and quantitatively support the reality of reaction of Eq. (3).

1.4. Self-trapped holes in a-SiO_2 have visible-range optical bands

Also noted in the uppermost timeline of Fig. 2 are publications by Kaya Nagasawa and coworkers [31,32] and by me [33], which do not treat Chernov et al.'s weak 1800-nm optical absorption band, but rather concern much stronger γ-ray-induced optical bands at 660 and 760 nm. In their ground-breaking pair of papers, Nagasawa et al. [31,32] characterized these bands in considerable detail but tentatively ascribed them to unidentified impurities.

Eleven years later I unexpectedly 'rediscovered' these same 660- and 760-nm bands in the course of a study funded by the US Department of Energy to develop rad-hard optical fibers for fusion-reactor diagnostics [34]. After studying them in greater detail, I proposed that Kaya's bands are due to STHs [35,36]. However, I did not then have isochronal anneal data to back up my claim. But in March 2002, near the end of my visiting professorship at Tokyo Institute of Technology, I managed to γ-irradiate two silica-based fibers at 77 K and record the induced optical spectra as functions of isochronal annealing and other treatments. I performed the data analysis while at Université de Paris 6. Those data pertaining to a fiber with a low-OH/low-Cl pure-silica core are represented by the open squares in Fig. 3 [33].

As indicated by both up and down triangles in Fig. 2, Katsumi Tanimura and coworker [37] achieved excellent correlations between the STH_2 ESR spectrum and an optical band at 574 nm, with both manifestations having been measured in the same (bulk) samples following exposure to 1-MeV electron pulses at 80 K. In Section 4, I will speculate on possible reasons why the Sasajima and Tanimura [37] did not observe the 660- and 760-nm bands in their experiment.

1.5. Self-trapped holes in a-SiO_2 have practical relevance – unforeseen by US science management

Asterisks at the ends of the four timelines in Fig. 2 signify that the research on these themes, until then still being performed in the United States, was terminated at these four respective moments. Each of these terminations was imposed by denial of funding by US-government-agency program managers and/or by decisions of managers in the researchers' direct chains of command. Whatever the wisdom of these decisions, Section 5 describes an event wherein the basic, *curiosity-driven* research that had been performed on STHs in a-SiO_2 saved NASA and the US commercial satellite industry a sum of money estimable to lie in the range ~$1M to ⩾$20M.

2. ESR spectra of STHs in a-SiO_2

Fig. 4(a) (solid curves) displays the ESR spectrum of low-OH, oxygen-rich Suprasil W1 following 100-keV X irradiation at 77 K [16,17]. This spectrum contains several overlapping components including E' centers [2,11,38,39] and a POR variant (principal peaks indicated by asterisks). The same POR variant – but not the E' centers – was also observed in a Suprasil W1 sample irradiated by 6.4-eV laser photons at 77 K, where the POR intensity was found to increase in strength one-for-one with the thermal bleaching of the STHs [40].

According to the dotted computer simulation of Fig. 4(a), the aggregate STH spectrum comprises a weighted sum of the three hypothetical STH components termed STH_1, STH_{mixed}, and STH_2, which are shown in Fig. 4(b)–(d), respectively [17]. These three simulated components are respectively based on the *g*-value distributions of Fig. 4(g)– (i). The average *g* values of STH_1 are very similar to those of the Ge trapped hole center in crystalline SiO_2 polymorph α quartz [10], while the *g* values of the other two proposed components are a priori consistent with expectations for other oxygen hole center variants.[1]

Although not illustrated here, I also determined the ^{29}Si and ^{17}O hyperfine coupling constants of STHs in isotopically enriched samples by means of computer line-shape simulations based on the models of Fig. 4(e) and (f) [17]. The methods and results of the hyperfine studies of Ref. [17] have been reviewed and updated recently [42]. Ab initio calculations [43] of the ^{29}Si hyperfine coupling constants of the STH_1 and STH_2 models of Fig. 4(e) and (f), respectively, have shown good agreement with the experimentally extracted values of Ref. [17], thus lending additional support to these models. Still, for reasons I will discuss below, I believe that ab initio calculations of the *g-value distributions* of STHs in a-SiO_2, when eventually performed, may prove to be of even greater value. (First-principles calculations of the *g* matrices of the E_1' and

[1] In a recent issue of this journal, Wang et al. [41] claim to have given 'a qualitatively experimental proof of the spectral *shape* (sic) of respective STH signals without any additional assumptions'. Based on what they actually did, it appears that these authors regard as an (undesirable) assumption the (standard) requirement that all viable component spectra obey *g*-value theory for oxygen hole centers. Moreover, these authors make additional assumptions of their own, including the ad-hoc notion that the shape of their bleached spectrum was identical with the spectral component(s) that determined 100% of the low field derivative maximum of their *unbleached* spectrum. The putative STH_1 and STH_2 components that Wang et al. [41] derived in this highly questionable fashion cannot be simulated by means of standard *g*-value theory for oxygen hole centers because these shapes exhibit spurious spectral features, as well as too much ESR intensity extending to high magnetic fields (corresponding to *g* values smaller than the free electron value). For these reasons, Wang et al.'s purported reanalysis of the STH ESR spectrum [41] serves to confuse, rather than clarify, our current state of knowledge.

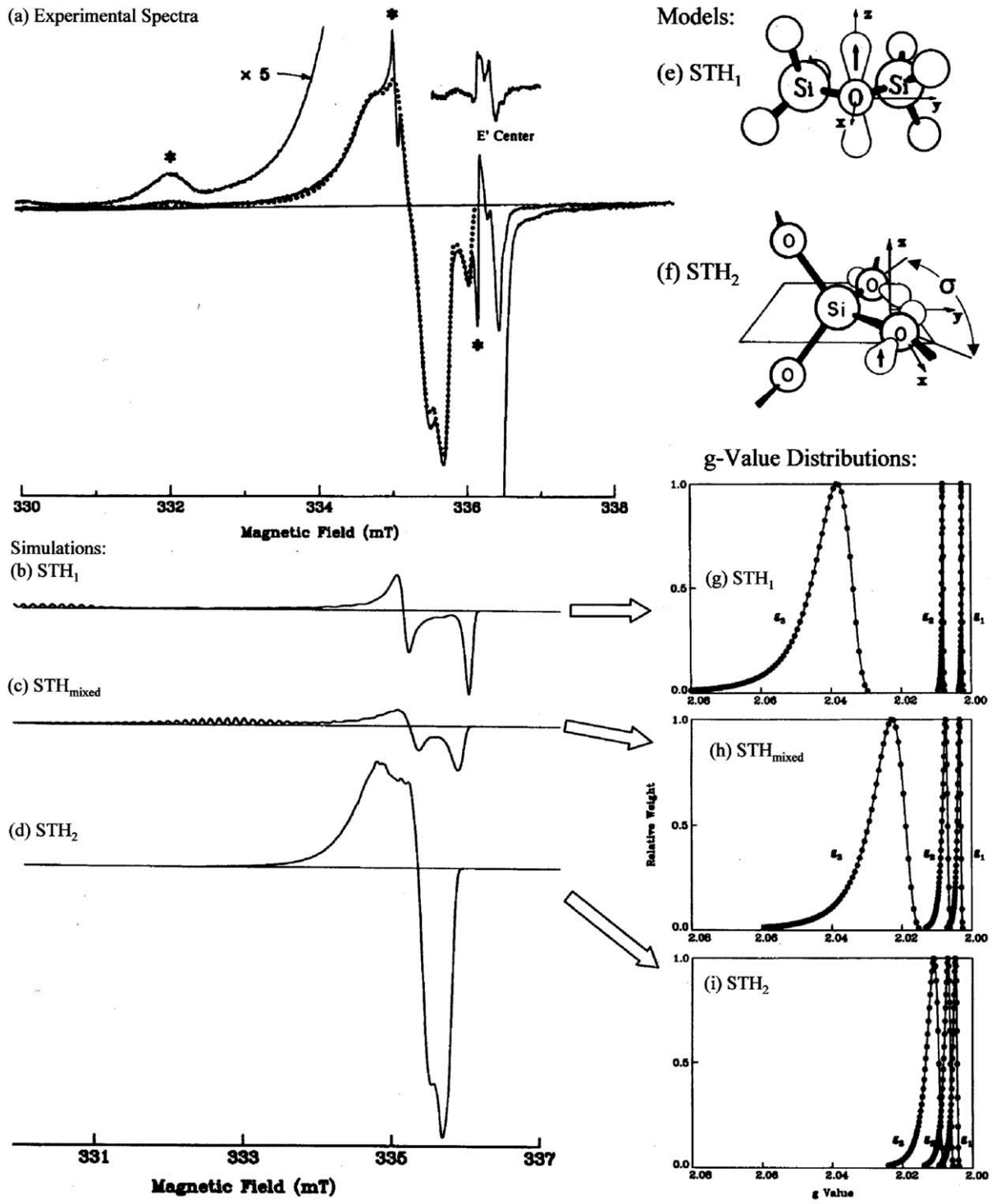

Fig. 4. Electron spin resonance spectrum, analyses, and model interpretations of self-trapped holes in a-SiO_2 [16,17]. (a) ESR spectra of bulk Suprasil W1 fused silica following X irradiation at 77 K. The spectral components for magnetic fields >336.1 mT are due mainly to E' centers. Asterisks mark features due to peroxy radicals. The employed microwave powers were 0.4 mW for the wide field scans of (a) and 0.2 μW for the vertically offset scan of the E'-center region only. The dotted curve is a computer simulation of the STHs only; it comprises a weighted sum of three inferred component spectra: (b) STH_1, (c) STH_{mixed}, and (d) STH_2. At the upper right are proposed structural models [17] for (e) STH_1 and (f) STH_2. The g-value distributions used in the simulations of (b)–(d) are shown in (g)–(i), respectively. (Adapted from [17].)

substitutional-phosphorus defects in α quartz have been recently reported [44].)

The skew-symmetric g-value distributions of Fig. 4(g)–(i) derive from *presumed* Gaussian distributions in certain electronic energy levels according to a well-defined mathematical transformation [2,17,42,45,46]. In the present case, all of the energy levels measurably affecting the g values fall within the valence bands of a-SiO_2 (see Fig. 5) [17].

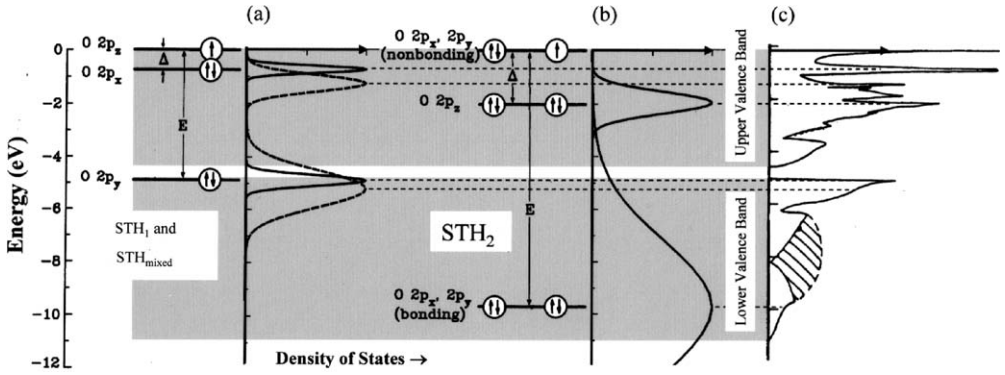

Fig. 5. Valence-band density of states (DOS) of a-SiO_2 [17] as revealed (a) by the g-value distributions of STH_1 (solid curves) and STH_{mixed} (dashed curves) and (b) by the g-value distributions of STH_2. The top of the valence band is taken to be at 0 eV. The ESR-determined best-fit-Gaussian sub-bands of (a) and (b) are evidently subject to 'selection rules' that cause STH_1 and STH_{mixed} to probe different parts of the valence-band DOS than STH_2. It should be noted that the DOS components pertaining to the *ground states* of the STHs are not measured, but they clearly must be confined to a narrow range immediately above 0 eV. The labeling of O 2p orbitals in (a) and (b) refers to the coordinate systems embedded in the models of Fig. 4(e) and (f), respectively. Curves (c) comprise a calculated DOS for 'amorphous crystobalite' [53]; (note the sharp peak at 0 eV). The shaded upper and lower valence bands pertain to the *calculated* DOS [53] (which places the intra-valence-band gap higher in energy than is experimentally determined [52]). The valence bands of SiO_2 comprise mostly O 2p , Si 3p, and Si 3s orbitals, with the silicon components vanishing near 0 eV. (Adapted from [17].)

2.1. g-Value theory of STH_1 in a-SiO_2

The principal-axis g-values for the model for STH_1 of Fig. 4(e) are given by [17]

$$g_3 = g_{yy} = g_e + 2\lambda/\Delta, \tag{4a}$$

$$g_2 = g_{xx} = g_e + 2\lambda M/E, \tag{4b}$$

$$g_1 = g_{zz} = g_e, \tag{4c}$$

where g_e is the free-electron g value (2.00232), λ is the spin-orbit coupling constant for the O^- ion (taken to be 0.014 eV [47]), Δ is the energy difference between the ground state of the unpaired spin (O $2p_z$) and the lower-lying non-bonding orbital of the same oxygen (O $2p_x$), E is the energy difference between O $2p_z$ and the mostly O $2p_y$ bonding orbital of Fig. 4(e), and M is the squared coefficient of the O $2p_y$ contribution to the bonding-orbital wavefunction. The model of Fig. 4(e) is essentially identical with that of the $[AlO_4]^0$ center in α quartz (well understood from angle-dependent ESR studies), except that in the $[AlO_4]^0$ case one of the two silicons is substituted by an aluminum (for a review, see [48]).

2.2. g-Value theory of STH_2 in a-SiO_2

Whereas the g-value theory of Eqs. (4) constitutes a textbook case (e.g., [49]), the theory pertaining to STH_2 is strikingly different [17,42]. Compelled by the fact that none of the three principal-axis g values was sufficiently close to g_e, I conceived of the STH_2 model of Fig. 4(f) and utilized the following equations which I had devised previously [50] for two of the principal-axis g values that would result in the case of a hole delocalized over two oxygens belonging to the same SiO_4 (or PO_4 [51]) tetrahedron

$$g_3 = g_{xx} = g_e + 2(\lambda/\Delta)\sin^2(\sigma/2), \tag{5a}$$

$$g_2 = g_{yy} = g_e + 2(\lambda/\Delta)\cos^2(\sigma/2). \tag{5b}$$

The parameter σ appearing in Eqs. (5) is the O–Si–O angle defined in Fig. 4(f). It was not immediately obvious which of the principal-axis directions of Eqs. (5) correspond to which of the axes labeled in Fig. 4(f). I determined the identities $g_3 = g_{xx}$ and $g_2 = g_{yy}$ of Eqs. (5) by a process of elimination [17]. As a result of this process, the principal-axis g-value distribution for STH_2 that falls closest to the free-electron value g_e takes the same form as Eq. (4b), i.e.

$$g_1 = g_{zz} = g_e + 2\lambda M/E, \tag{5c}$$

where the mean value of E in Eq. (5c) is *empirically* larger than the value that yields g_2 in the case of STH_1, Eq. (4b), assuming approximately equal values of M.

2.3. STH g-value distributions as probes of the valence-band density of states of a-SiO_2

As a matter of convenience, I performed all of the trial ESR spectral simulations of Ref. [17] using a 'generic' skew-symmetric g-value distribution (derived for an arbitrary Gaussian distribution in E or Δ) that I shifted and stretched as a way of optimizing my spectral fits. When I arrived at the final fit of Fig. 4(a) (dotted curve), I determined by iteration a set of Gaussian energy-level distributions that lead to g-value distributions closely approximating the manipulated generic ones of Fig. 5(g)–(i). These 'back calculated' Gaussian energy-level distributions are shown in Fig. 5(a) and (b), where for this purpose I arbitrarily used $M = 1$ in Eqs. (4b) and (5c), since I had no means of calculating the (likely smaller) true values of M.

Since all of the energy levels involved in the g-value theory of Eqs. (4) and (5) fall in the valence band of a-SiO_2, I decided to compare the best-fit energy-level distributions of Fig. 5(a) and (b) with the density of states (DOS) of silica. For this purpose I selected a calculated DOS in place of an

experimental one, because the experimentally determined ones are artificially broadened (masking any sharp peaks) and somewhat dependent on experimental conditions [52]. So, in Fig. 5(c) I display an early semiempirical DOS calculation for 'amorphous crystobalite' by Pantelides and Harrison (PH) [53]. I have summarized the methods and significance of the PH calculation in a review of the electronic structure of SiO_2 [52], where I also compared the PH results with experimental measures of the valence-band DOS of silica.

The spectroscopic data that I reviewed in Ref. [52] hint that the valence band of a-SiO_2 may consist of two subbands with a gap between them, which is not quite resolved experimentally. The PH calculation in fact shows a gap (as does a non-empirical calculation by Schneider and Fowler [54] for the valence band of idealized β cristobalite). However, the PH theory [52] placed the gap ~1 eV higher than the position of the gap suggested experimentally. Thus, the remarkably good correspondences between the *g*-value distributions of Fig. 5(a) and (b) and the PH DOS of Fig. 5(c) would be at least partially fortuitous for this reason alone. More significantly, however, the mean values of E portrayed in Fig. 5 are too large by as much as a factor of 2, due to my arbitrary decision [17] to take $M = 1$ in my calculations of the σ-bonding-orbital energy-level distributions. Indeed, if STH_1 and STH_{mixed} are correctly interpreted as conventional small polarons [4,8], the relaxations associated with polaron formation should have weakened the O $2p_y$ bonding orbitals at the sites of the trapped holes, causing their energy levels to rise upward toward the valence band top relative to the *defect-free* DOS.

In Fig. 5, STH_2 tells a very different story than STH_1. It can be seen in Fig. 5(b) that the best-fit mean value of E pertaining to Eq. (5c) (with M arbitrarily set equal to 1) is virtually equal to the entire depth of the valence band of SiO_2.[2] (NB As part of the semiempirical nature of the PH calculation, there was an adjustable parameter that was used to force the calculated valence-band DOS to have the same overall width, ~11 eV, as the experimental one [52,53].) Thus, the value of E obtained from ESR spectral fitting suggests that there is less polaronic relaxation in the case of STH_2 than in the case of STH_1. Moreover, the value of σ used in Eqs. (5a) and (5b) to obtain the best fit of STH_2 was 107.5° [17], that is, within experimental error equal to the tetrahedral angle of 109.47°. Hence, two independent aspects of the STH_2 g matrix of Fig. 4(i) each suggest that little relaxation occurs at STH_2 trapping sites.

If it should turn out that the STH_2 site is only slightly relaxed after hole trapping, this fact could compel a paradigm shift in the theory of polarons in glasses. This is because all carriers as severely localized as the hole in the STH_2 model of Fig. 4(f) have been regarded as *small polarons* by both Mott [8] and Emin and Bussac [55] – and small polarons are currently considered to be synonymous with trapping sites involving significant atomic displacements from their equilibrium positions *consequent to the hole being present* [55]. In any event, the theoretical approach of Emin and Bussac [55] (which treats small polaron formation in covalent glasses with bond-angle variations) is appropriate to calculating the energetics of STH_2, whereas the original theory of Anderson [7] (which assumed randomly positioned impurity ions) is not. Until theoretical calculations specific to STH_2 are actually done, I am inclined to view the STH_2 trapping sites as pre-existing in a-SiO_2, that is, having pre-existing energy levels lying above a pre-existing valence-band mobility edge as schematically illustrated in Fig. 1.

3. Recent evidence that strained bonds favor STH formation

Whether or not they are small polarons in the classical sense, STHs in any amorphous material have to be fundamentally different from self-trapped holes in crystals. This is because, whereas every self-trapping site in a crystal is identical to every other, the trapping sites in any glass are surely characterized by a continuum of *pre-existing* trap depths. In partially covalent glasses, this continuum of well depths is generally attributed to a continuum of 'strained bonds'. Indeed, bond strains might be viewed as the origin of band tails extending upward into the energy gap from the valence band. Metastable hole trapping near the tops of such tails would then imply the existence of mobility edges (Fig. 1) as proposed by Mott [8,9] and possibly observed directly by Chernov et al. [29].

But is there truly a link between strained bonds and STHs? Well, Yamaguchi et al. [56] decided to check this notion by measuring the yields of STHs induced at 77 K by identical ArF-laser irradiations of a series of pure-silica samples that were identical all respects other than having differing imposed values of the fictive temperature, T_f. The striking results of this study are shown as the open squares in Fig. 6.

In addition to lowering T_f by annealing, it is known that bond strain in silica glasses can also be reduced by replacing some of the bridging oxygens with non-bridging monovalent species, such as OH^-, Cl^-, or F^-. Accordingly, Wang et al. [57] undertook a study of the dependence of STH yields (presumably under the same experimental conditions as the experiment of Yamaguchi

[2] The 'best fit' Gaussian distribution in E illustrated in Fig. 5(b) clearly exceeds the experimental valence-band width below −11 eV. Although obviously incorrect, this discrepancy does not discredit the approach, since for consistency I imposed Gaussian energy-level distributions when carrying out *all* of the fits of Fig. 4(a) [17]. My 'final' STH spectral simulation (dotted curve in Fig. 4(a)) is in fact is not perfect. Thus, it remains conceivable that an equally good, or better, fit might be obtained if the energy-level distribution corresponding to the splitting E of Fig. 5(b) were to be constrained to resemble the *experimentally determined shape* of the lower valence band of SiO_2, rather than the overly broad Gaussian that I used.

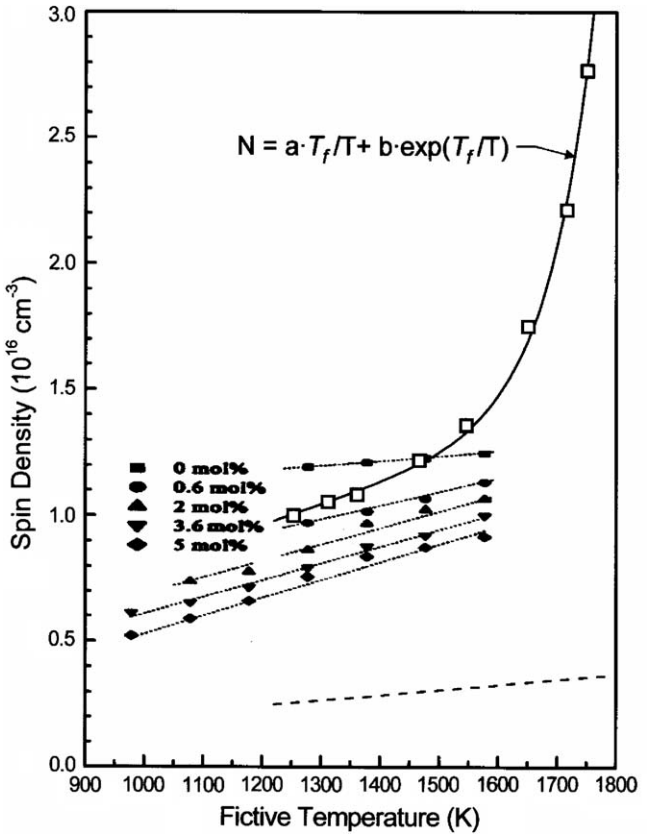

Fig. 6. STH spin densities at 77 K for fixed-dose ArF-laser irradiations of pure-silica (squares) and F-doped silicas (other symbols) as functions fluorine doping and/or fictive temperature T_f. Open squares are data from Ref. [56]; solid symbols and dotted lines are taken from Ref. [57]. The solid curve passed through the open squares was fitted by the present author using the indicated algorithm with the following parameterization: $a = 0.0616$, $b = 1.85 \times 10^{-10}$, and $T = 77$ K. The long-dashed curve is the result of setting $T = 300$ K, while keeping the same values of a and b. A possible meaning of this mathematical relation is proposed in the text.

et al. [56])[3] except that both T_f and the degree of fluorine doping were varied. These results are shown as the solid symbols in Fig. 6.

Since fluorine is not expected to compete as a hole-trapping entity, and all experimental evidence to date indicates that it does not in fact trap holes (e.g., [34,58]), the experiments of [56,57] taken together show that any heat treatment or doping of silica glass known to reduce bond strain *also* reduces the yield of STHs under otherwise fixed experimental conditions. Thus, the connection between strained bonds in silica and the STH-defined band tails and mobility edge at the top of the valence band (Fig. 1) now rests on a more secure foundation.

In Fig. 6, I have fitted the data of Yamaguchi et al. [56] to an algorithm that I derived by 'cut and try' (solid curve). Based on the form of this fitting function (see figure) *and the fact that the reference temperature T turns out to be the experimental sample temperature*, I tentatively interpret its meaning as a measure of the density of hole-trapping states lying higher than $\sim kT$ above a mobility edge near the top of the valence band in a-SiO_2 (k is Boltzmann's constant). If this interpretation is correct, then the long-dashed curve at the bottom of Fig. 6 (obtained by using $T = 300$ K with the same values of a and b) predicts the density of STH states lying $\geqslant kT$ above the mobility edge at room temperature.

As I reported in [42], room-temperature-stable STHs have been identified by ESR in an isotopically enriched bulk silica sample that was kindly densified for me by Rod Devine. (Rod's methods and some of his discoveries relating to defects in densified silicas are described in [59,60].) Room-temperature-stable STHs have also been detected electrically in thin silica films on silicon [22,42] and optically in a pure-silica-core fiber [33] – assuming that Nelson Saks' trapped positive charge [22] and my the 660 and 760 nm bands [33] were truly STH manifestations (see evidence in Section 4).

4. Optical bands attributable to STHs

4.1. Optical bands recorded in γ-irradiated optical fibers

Fig. 7 [36] illustrates the induced optical bands (including the 660- and 760-nm bands) in a low-OH-high-purity-silica-core optical fiber at selected moments during in situ room-temperature γ-irradiation at 1 Gy(Si)/s, in the dark (except for white light ~5 μW injected for ~5 s during each spectral acquisition). Using a multi-channel, dual-beam, charge-coupled-device spectrometer that I describe in

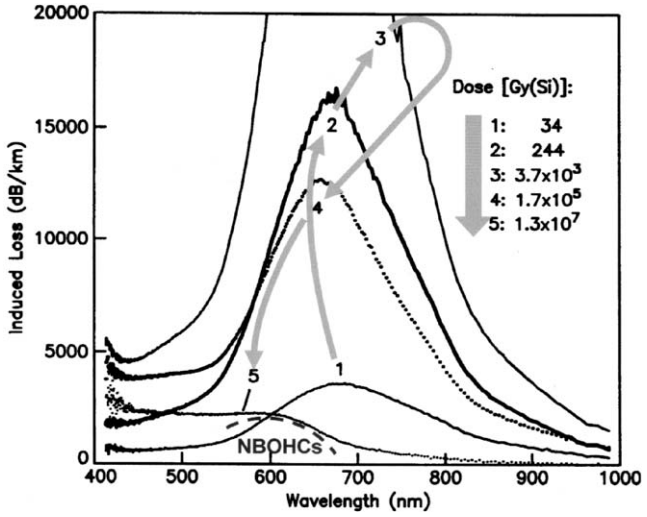

Fig. 7. Induced optical absorption bands in a low-OH-pure-silica-core optical fiber recorded in situ during γ irradiation at a dose rate of 1.0 Gy(Si)/s at 27 °C in the dark (except for injection of white light ~5 μW for ~5 s during frame grabs). Gray arrows indicate spectral evolution with continuously increasing dose. (After [35].)

[3] Although Refs. [56,57] have two authors in common (normally implying consistent methods), there is a significant unexplained discrepancy between the STH-yields-versus-fictive-temperature data for the pure-silica samples of [57] (solid squares in Fig. 6) and the corresponding data of [56] (open squares).

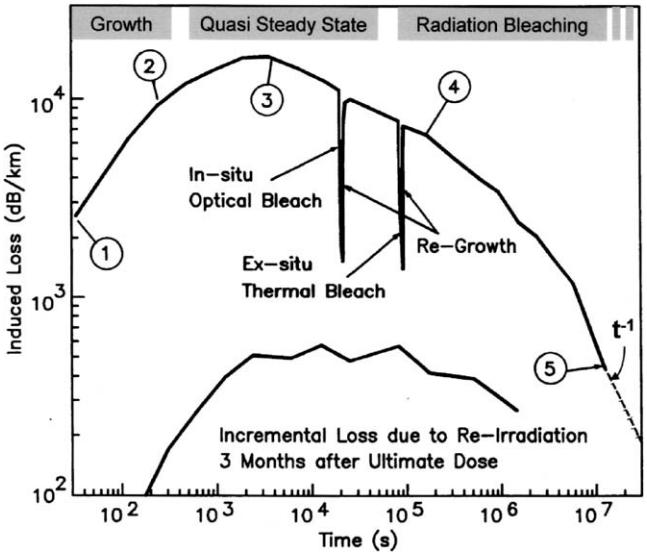

Fig. 8. Kinetic behaviors of γ-ray-induced optical absorption measured at 760 nm in a low-OH-pure-silica-core optical fiber irradiated at 27 °C in the dark, except for injection of white light ~5 μW for ~5 s during each frame grab (and continuously during the in situ optical bleach). All data were recorded in situ (fibers placed next to γ-ray source) except for the indicated ex situ (radiation off, light off) thermal bleach. Circled numbers correspond to the numbered spectra in Fig. 7. The dashed extrapolation for times longer than 10^7 s is proportional to reciprocal time. A second irradiation conducted 3 months later (lower curve) shows that the apparent degree of radiation-induced bleaching corresponding to point No. 5 in the upper curve amounted to a permanent 'hardening' against subsequent radiation-induced absorption at the same wavelength. Accumulated doses in Gy(Si) are approximately equal to the running time in seconds. (After [35].)

Ref. [34], I simultaneously recorded remarkably similar spectra for a low-OH-*F-doped*-silica-core fiber during the same experimental run (spectral and kinetic data for this fiber are given in [35]). These two 200-μm-core fibers had been fabricated under identical conditions at the Fiber Optic Research Center in Moscow with 240-μm-diameter F-doped-silica optical claddings and hermetic aluminum jackets [61]. The low-OH-high-purity-silica core rod was KS-4V glass (<0.2 ppm OH, <20 ppm Cl) of Russian origin, while the F-doped-silica core rod (4 ppm OH, 0.54% F) was an experimental product of Japanese industry [34]. The aluminum jackets ruled out color center bleaching by room light admitted laterally, and they also eliminated the possibility of color center reactions with hydrogen that can be radiolytically released from polymer jackets [62]. NB I used lengths of the same two fibers for the liquid-nitrogen-temperature γ irradiations that provided the first strong evidence [33] that the 660 and 760 nm bands arise from STHs (open squares in Fig. 3).

Fig. 8 [36] illustrates the time evolution of the absorption at a single selected wavelength (760 nm) for the KS-4V-core fiber during irradiation at room temperature. Here, the circled numbers on the upper curve correspond to the numbered spectra in Fig. 7, and the dose is very nearly equal to the running time in seconds. There are two downward transients illustrated in Fig. 8, one corresponding to an in situ optical bleach (with the radiation still on)[4] and the other to an ex situ thermal fade. I provide detailed kinetic data for these transients in Ref. [63], where I also show that they can be accurately fitted by using fractal-kinetic formalisms. The easy optical bleaching is typical of electrically charged defects [1].

The ex situ thermal decay shown in Fig. 8 shows that the quasi-steady-state condition at intermediate doses is due to an quasi-equilibrium between the rate of carrier creation and their rate of thermal destruction – that is, the observed flattening of the growth curve was *not* due to saturation of all available trapping sites, or to radiation-induced detrapping. This means that the quasi-steady-state loss should be higher at higher dose rates, and I have experimentally verified this [63]. A surprising result is that (independent of dose rate! [35,63]) a 'radiation-stimulated reconfiguration' (RSR) of the glass structure takes place at times longer than $\sim 10^5$ s, causing the induced absorption to irreversibly decrease *during irradiation* according to standard (non-fractal) second-order kinetics (proportional to t^{-1} for long irradiation times t: Fig. 8). NB The data of Fig. 6 in conjunction with other new evidence summarized in Section 3 lead me to speculate that the RSR phenomenon might alternatively be described as *radiation-stimulated reduction in fictive temperature*.

4.2. Optical bands recorded for pulse-electron-irradiated bulk silica samples

Sasajima and Tanimura [37] carried out both optical and ESR studies of three high-purity silica glasses following pulsed 1 MeV electron irradiations at 80 or 6 K. Their samples included one with <1 ppm of either OH or Cl, one with 1000 ppm OH and <1 ppm Cl, and one being the same Suprasil W1 material that I had used to obtain the spectrum of Fig. 4(a). They took ESR spectra using virtually the same spectrometer settings as I used to obtain the spectrum of Fig. 4(a) while recording optical spectra in the range 200–1000 nm. These data were then examined as functions of dose and various isochronal thermal anneals and isothermal optical bleachings. Fig. 9 exhibits the linear correlation found by Sasajima and Tanimura between the STH_2 ESR intensities and the induced optical density at 2.2 eV measured following growth (open circles), optical

[4] In Ref. [33] I present data for ex situ (radiation *off*) white-light optical bleaching of the induced absorption measured at 660 nm for the F-doped-silica-core fiber following γ irradiation of part of the fiber at 77 K (and other parts at 290 K, where thermal bleaching should have been proceeding in parallel). Surprisingly, these data could be fitted to ±0.6% accuracy at each of the six data points using standard (non-fractal) *second*-order kinetics. This fit extrapolated to zero absorption at infinite time – implying that bleaching of the induced bands in both the warm and chilled parts of the fiber was dominated by the light alone. Experiments of this nature need to be repeated, since by contrast, Wang et al. [41] used a *fractal first*-order kinetic formalism to fit (with unspecified accuracy) their data for optical bleaching of laser-induced-at-77-K STH ESR spectra of bulk silica samples.

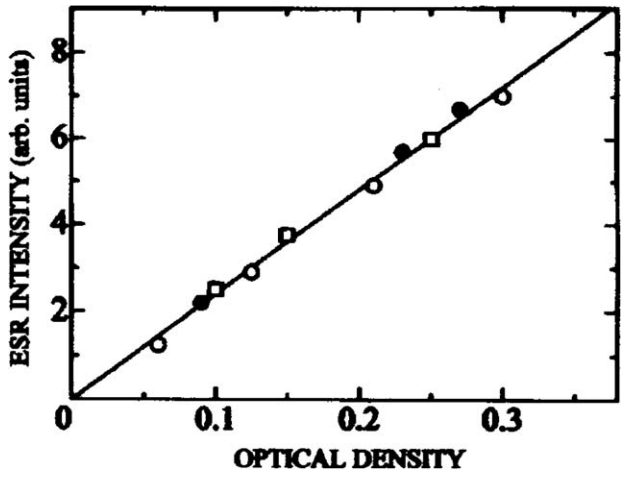

Fig. 9. Correlation between induced optical density at 2.2 eV and the induced ESR intensity of STH_2s recorded for the same 1-MeV-pulsed-electron-irradiated silica sample. The irradiation and the optical measurements were carried out at 80 K; ESR spectra were recorded at 77 K without warming. This sample ('SZ') contained less than 1 ppm of either OH or Cl. Meanings of the different data points are mentioned in the text. (From Ref. [37].)

bleaching (open squares), and thermal annealing (solid circles). Experiments using linearly polarized bleaching (see Fig. 10) placed this STH_2 band more precisely at 2.16 eV.

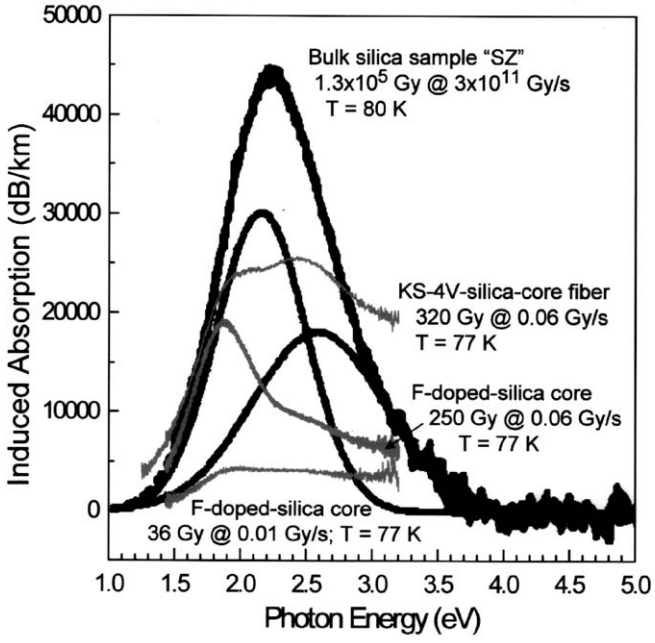

Fig. 10. Dichroic absorption spectrum (thick noisy black curve) induced by polarized red light in pure-silica specimen 'SZ' subjected to pulse irradiation by 1 MeV electrons at 80 K (from Ref. [37]). The two smooth black curves comprise a two-Gaussian fit [37] that was further justified by separate experiments on a Suprasil W1 sample also displaying bands at 2.16 and 2.60 eV – which were shown [37] to disappear around 140 K and 180 K, respectively, as in the cases of STH_2 and STH_1, respectively (see Fig. 3). Gray curves are optical spectra induced in pure- and F-doped-silica-core fibers by low-dose-rate, low-total-dose γ irradiations at 290 K [33]. The y-axis scaling pertains only to the gray curves; the peak of the black curve corresponds to an absorption of about 400 000 dB/km.

These experiments, when compared with data from their annealing experiments on Suprasil W1 (which were in turn were similar to my STH_2 and STH_1 annealing data of Fig. 3), permitted these workers to resolve a weaker band at 2.60 eV and logically attribute it to STH_1.

Sasajima and Tanimura [37] saw no evidence for the 660 or 760 nm bands. Does this mean that these are not STH bands, notwithstanding the correlation I have shown in [33] (Fig. 3)? Well, we cannot be sure without taking full account of the differences between their experimental conditions and mine. First, Sasajima and Tanimura employed an ionizing dose rate about eleven orders of magnitude larger than mine. However, my current guess is that the dose rate may be irrelevant when all samples are held near 77 K during irradiation. Second, there was the difference in total doses, theirs being 130 kGy and mine falling in the range 35 and 320 Gy. I think this could be a factor, since the first holes to trap at low doses may be at sites with the largest trapping cross sections. Indeed, there is a dose dependence of the shapes of the induced optical absorption spectra that I recorded in the low-dose range (Fig. 10, gray curves). Nevertheless, I suspect that the main issue will turn out to be *fictive temperature*.

Probably all commercial suppliers of bulk optical-grade silicas anneal their materials in the glass transformation range to establish thermal homogeneity. In so doing, they set a fictive temperature (likely to be in the range 1000–1200 °C, because the requisite anneal can be accomplished in about a day's time [64] without risk of crystallization). By contrast, silica-based optical fibers are quenched from draw temperatures ~2000 °C (1940 °C in the case of my KS-4V and F-doped-silica core fibers[5]) at rates ranging from 3000 to 30 000 °C/s for the 125-μm-diameter fibers of Ref. [65] (~300 °C/s in the cases of my 240-μm-diameter fibers[5]). Kim et al. [65] have measured the fictive temperatures of the pure-silica claddings of 125-μm-diameter single-mode fibers versus depth from the surface, finding T_f to lie in the range ~1620–1650 °C irrespective of quench rate or distance beneath the surface from ~2 to 40 μm. These workers [65] recorded lower values of T_f for the Ge-doped cores of their fibers (~1150–1300 °C) and for F-doped inner claddings (~1400–1600 °C). Thus, my KS-4V and (0.54 mass%) F-doped silica core fibers could have had fictive temperatures as high as 1600 and 1500 °C (1873 and 1773 K), respectively.

Referring to Fig. 6 (open squares), it can then be supposed that the parts of my fibers of Ref. [33] that were held at 77 K could have had STH yields more than three times higher than those of Sasajima and Tanimura's [37] bulk samples. Yet the STH *yield* is almost certainly not the main issue when the subject is STH *optical bands*. Rather, I believe that the dominant effect of T_f should be on the *oscillator strengths*, f. It can be supposed that the oscillator

[5] This information was kindly provided by Professor K.M. Golant, Director, Business-Unitech Co. Ltd, MSU Science Park, Bld. 75, Leninskie Gory, 119992, Moscow, Russia.

strengths of STHs should be similar to those of other oxygen-associated hole centers in silica, i.e., 0.00054 [66,67] or 0.00028 [68] for the NBOHC and 0.00057 [67] for the POR. These values of f are low because they pertain to symmetry forbidden O 2p → O 2p transitions. Thus, significant bond strains associated with high fictive temperatures seem more likely to increase f than to lower it. Moreover, the STHs certainly have a continuum of forbidden transitions extending downward into the valence band, and it seems possible that the oscillator strength of any one of these could be raised from virtually zero to, say, 0.0005 for STHs mainly localized at strained-bond-stabilized trapping sites. In this context, it is worth recalling that Harari et al. [30] photo-depopulated X-ray-induced positive trapped charges in an a-SiO_2 thin film (likely to have contained many strained bonds) with peak efficiency for photons near 1.6 eV (775 nm).

Since the bands I reported in Ref. [33] and reproduce here in Fig. 10 (gray curves) are seen to fall within the envelope of Sasajima and Tanimura's 2.16 and 2.60 eV bands (which they have reliably associated with STH_2 and STH_1, respectively), I suggest that these two broad Gaussian bands may actually be composed of two series of narrower Gaussian bands, perhaps corresponding to sharp peaks in the upper-valence-band DOS (see Fig. 5(c)). Indeed, in [35] I resolved distinct Gaussian bands centered at 1.37, 1.58, and 1.83 eV with halfwidths of 0.22, 0.22, and 0.44 eV, respectively, induced in the KS-4V-core fiber during γ irradiation at ambient temperature.

5. Relevance to industry

Those of us lucky enough to have made our livings by performing curiosity-driven basic research have frequently been non-plussed by the question: "What is the relevance of your work to the 'real world'?" In response to such challenges, I have decided to make public the following cautionary tale.

5.1. The mystery of the tumbling satellites

By late 1998, a durability problem was detected in AlliedSignal ring-laser gyros (RLGs) being tested for Space Imaging's Ikonos 1 spacecraft [69]. The previously reliable RLGs, designed to operate in space for 20 years, now seemed to be failing in orbit after only one year! Accordingly, all scheduled satellite launches involving these particular RLGs were put on hold – at costs ~$15 000–$100 000 per day per launch vehicle – pending solution of the problem. Affected were Space Imaging, NASA's Far Ultraviolet Spectroscopic Explorer (FUSE) satellite, Orbital Sciences (as a NASA contractor), and Iridium LLC (whose 8 + tumbling satellites [70] out of their ~77-satellite constellation likely gave the first indications of high RLG failure rates). Launch vehicle manufacturers, such as Lockheed Martin, were also deeply concerned.

I was summoned by NASA Goddard Space Flight Center as a pro-bono government consultant to attend a problem-solving meeting at AlliedSignal's plant in Teterboro, New Jersey, on 20 November 1998. After a half day of presentations and discussions by managers and scientists, I asked the key question: 'What is the purity of the silica sputtering target used for depositing the highly reflecting SiO_2/TiO_2 stacks on the RLG mirror surfaces?' The answer came back: 'Whatever the target manufacturer provided'. As I suspected, the target turned out to be fused natural quartz. I suggested that the RLG failures most likely resulted from aluminum-impurity-related color centers (analogous to the $[Al]^0$ center in smoky quartz [48,71]) induced in the a-SiO_2 top-surface coatings on the RLG mirrors by action of 20-eV photons concomitantly emitted by the HeNe laser plasma. Given that $[Al]^0$ centers give rise to a 'gray' absorption in the range ~300–1000 nm [71,72] and that the HeNe laser line is at 632.8 nm, I proposed replacing the sputtering target with Al-free fiber-optic-grade synthetic silica.

Nevertheless, RLGs employing new mirrors fabricated with aluminum-free silica still failed accelerated tests. I was able to explain these failures as likely artifacts of the 660-nm STH absorption, which, like the $[Al]^0$ bands, strongly overlaps the HeNe laser line (see Fig. 7). However, *unlike* the $[Al]^0$ bands, the STH bands attain quasi-steady-state absorptivities that are larger at higher dose rates [63], *inevitably yielding false positives in accelerated tests*! I was also able to point out that this band irreversibly *disappears* in proportion to t^{-1} for irradiation times $t \geqslant 10^6$ s (Fig. 8), so it could be predicted that the RLG performance should *improve* with long-term, low-dose-rate operation! The scientific members of the troubleshooting team were convinced by my arguments. However, before any defective component could be declared re-qualified for space deployment, the team was required by industry protocols to devise a further ground test to justify discounting an accelerated-test failure.

So I was asked to suggest a separate experiment that might be performed to corroborate what we all knew to be essentially correct. In retrospect, if I had been mentally alert, I could have pointed to the fact that the 660-nm band is metastable and that by merely shutting off the accelerated test for a few hours, the RLG would *initially* run 'as good as new' when restarted at the accelerated power level (see ex-situ thermal bleaching transient in Fig. 8). However, I failed to think of this at the time and instead mentioned that I had tentatively ascribed the 660- and 760-nm bands to STHs and that I might look for the ESR signals to determine their presence in thin films manufactured in the same way as the new mirror surfaces.

Even though I was concerned that any STHs might anneal out in one day's time, the troubleshooting team sent me some newly sputtered films by overnight courier. When I put these in my ESR spectrometer at the Naval Research Laboratory, I recorded the results of Fig. 11 – which I interpreted as 'resembling distorted STH spectra' (maybe

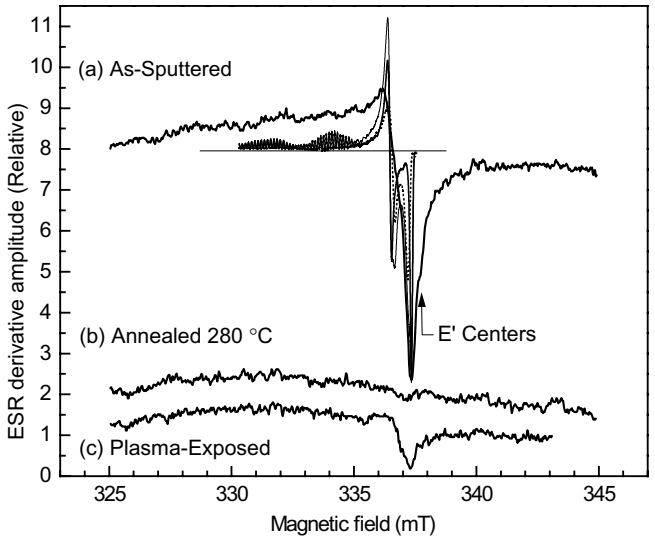

Fig. 11. X-band ESR spectra recorded under identical high-gain spectrometer conditions for sputtered high-purity SiO_2 films on silicon substrates (thick curves). (a) As sputtered. (b) After annealing to 280 °C. (c) After 280 °C anneal and exposure to high-intensity HeNe laser plasma. For comparison, the thin curves in (a) are reproductions of the simulated STH_1 (solid) and STH_{mixed} (dashed) spectra of Fig. 4(b) and (c), respectively. The magnetic-field registration of these STH components tentatively assumes that the shoulder marked by the arrow is due to *E′* centers. Note that the simulated curves do not constitute an attempt to *fit* the spectrum of (a); any serious attempt to do this would require g_2 distributions with much larger widths than those of Fig. 4(g) and (h). The broad background which characterizes spectrum (b) is likely to have been determined by microwave-cavity contamination; presumably this same background underlies (and distorts) the other two spectra.

an extreme case of STH_{mixed}). These spectra are definitely not due to $[Al]^0$ centers in glassy silica, which exhibits unmistakable ^{27}Al hyperfine structure [73,74].

The 'additional ground test' of Fig. 11 (although circumstantially based on my *then unsupported* association of the 660-nm band with STHs) was regarded as having satisfied industry protocols. All RLGs were immediately refitted with mirrors coated with Al-free silica films, and launches of all satellites employing AlliedSignal's Attitude Control System were rescheduled into the earliest possible slots (e.g., 24 June 1999 for FUSE and 24 September 1999 for Ikonos [75]). To my knowledge, in the past six years there have been no reports of the corrected RLGs failing in space.

5.2. What went wrong?

By 1998, the ring-laser-gyro was a mature technology that had been in practical use for two decades [76]. Why then would RLGs suddenly start failing at that time? The answer is that corporate memory for scientific details is short, since scientists assigned to original development programs are routinely reassigned, laid off, or retired. Thus, it becomes inevitable that seemingly innocuous engineering changes, un-vetted by scientists cognizant of the fundamental issues, can occasionally prove disastrous. Moral: Good basic science must be kept alive, not just to spark the technologies of 20 years in the future, *but also to assure the survival of technologies that are already 20 years old!*

6. STHs in a-SiO_2: Where do we go from here?

We now know that STHs can be created in a-SiO_2 by ionizing radiations (including ultraviolet photons [40,41,56,57]) and that they exist in two principal varieties that can be discriminated by ESR (Section 2 and [17]). We know too that STHs have optical absorption bands in the visible range/near infrared (Section 3 and [33,37]) and mid infrared [29], and we have good evidence that some STHs are metastable at room temperature (see Section 3 and Fig. 11). We also know that certain of the induced optical absorption bands likely associated with STHs in a-SiO_2 can be suppressed by pre-irradiation (Fig. 8 and [35,36,63]), presumably due to reconfigurations of the glass structure that affect the number and/or oscillator strengths of the sites available for hole self-trapping (the phenomenon I have termed RSR in [63] and Section 3). But there remain gaps in our knowledge which need to be filled.

6.1. Uncertainties about the optical bands

One of the first things that my contemporaries and I learned as newly minted physicists was that 'a correlation is not a proof'. Still, in my personal view, the multi-facetted ESR-optical correlation established by Sasajima and Tanimura [37] (Fig. 9) is as good as a proof that STH_2 has an optical band at centered 2.16 eV. By contrast, my own results (Fig. 3 and [33]) indirectly correlating the 660-nm (1.88 eV) and 760-nm (1.63 eV) bands with STHs are weaker than a true proof – although I attach significance to the fact that the 660 and 760 nm bands must be due to *some* metastable color center(s), whereas the STHs are the only paramagnetic species in pure, or impure, silicas known to anneal in the 140–220 K temperature range (see references that I cite in [33]). This situation needs to be clarified by performing more and better ESR and optical studies on optical fiber samples, analogous to what was done in [37] in the case of bulk samples.

6.2. How pervasive are reactions of STHs with interstitial atoms?

I think that my proposition that STHs react with radiolytic atomic hydrogen to form protons, Eq. (3), has been adequately proven (see [20] for a review of the early evidence). More recently I have postulated that STHs should *also* react with interstitial Cl^0 (which is known to be radiolytically created in silicas with high chloride contents [77]) – and also with interstitial atomic oxygen. In fact, Masafumi Mizuguchi and I [67] gathered ESR and optical data for γ-irradiated low-OH/low-Cl, (and F-doped) silicas which caused us to agree with Skuja and Güttler's [78] conclusion

that O^0 is the *dominant* interstitial atom resulting from γ radiolysis of low-OH silica at room temperature.

However, a discrepancy between Mizuguchi's ESR data and my optical data (regarding isochronal anneals performed on samples exposed to similar doses but at different dose rates), led me to propose in [67] that this discrepancy may have been due to (dose-rate-dependent) reaction of O^0 with STHs to form small peroxy radicals (SPORs)

$$\equiv\text{Si-}\dot{\text{O}}\text{-Si}\equiv + \text{O}^0 \rightarrow \equiv\text{Si-}\underset{}{\overset{\overset{\cdot}{\text{O}}\,|}{\text{O}}}\text{-Si}\equiv, \tag{6}$$

where the first entity on the left-hand side of Eq. (6) represents STH_1 and the di-oxygen species on the right-hand side is a SPOR. The existence of SPORs in a-SiO_2 was originally proposed by Edwards and Fowler [79], who also calculated their structure and energetics.

More recently, Kajihara, Skuja, and coworkers [80,81] demonstrated the role of mobile interstitial atomic oxygen in the interconversion of PORs, NBOHCs, and peroxylinkages (≡Si–O–O–Si≡) in silica following F_2 laser photolysis of deliberately introduced interstitial O_2 molecules. However, these workers did not make a distinction between the (bridging) SPOR and the singly bonded POR, nor did they consider the possible role of STHs in the phenomena they have reported.

6.3. Does F_2 laser irradiation create STH/self-trapped-electron pairs?

Possibly the reason that STH interactions with interstitials were neglected in Refs. [80,81] is because the F_2 laser quantum (7.9 eV) lies sufficiently far below the photoconductivity edge in a-SiO_2 (∼9 eV [52]; see Fig. 1) that virtually all STHs would be formed in intimate pairings with immobile electrons. If so, virtually all of these e–h pairs would rapidly form self-trapped excitons (STEs) and decay in times short compared to the time required for diffusing O^0 to reach these sites. However, this notion needs to be experimentally tested.

6.4. What is the mechanism of the radiation-stimulated reconfiguration?

In general, the physical reason for the RSR phenomenon (the disappearance of 660 and 760 nm bands according to a t^{-1} time dependence for irradiations continuing longer than $\sim 5 \times 10^6$ s: Fig. 8) is still unknown. Within the accuracy of the available data [35,36,63], this particular time dependence implies a standard (non-fractal) second-order kinetic process. I have speculated in [35] that a conceivable second-order process might be strained bonds that migrate when they become the sites of self-trapped excitons (STEs) and that net strain relief might be accomplished when two migrating strained bonds meet. If the data of Fig. 3 are accepted as sufficient evidence to assert that 660 and 760 nm bands arise from STHs, RSR would be logically interpreted as a reduction in the number of possible hole self-trapping sites with increasing irradiation time. What are these sites? Well, the increasing STH yield with increasing fictive temperature data reported in [56] (Section 3 and Fig. 6) points directly to strained bonds. But however appealing this model may appear, it is far from proven.

Alternatively, the reaction of Eq. (6), if taking place in a time interval when STHs and interstitial oxygen atoms are present in roughly equal numbers, could account for the disappearance of STH trapping sites following the observed kinetics within present experimental accuracy. This notion could be proven (or disproved) by a careful ESR search for SPORs in a-SiO_2 samples that have been irradiated for times longer than $\sim 10^6$ s ca. 300 K.

6.5. Pulsed radiolysis of pure-silica core fibers

Studies of the responses of silica-based optical fibers to high-dose-rate pulsed radiolysis have been conducted since the early 1970s, mostly with military applications in mind. Nowadays such studies have been redoubled in the hope/expectation of using silica-based fibers for diagnostics of plasmas generated by super-large lasers (e.g., the US National Ignition Facility, NIF, and the European Laser Mégajoule, LMJ) or tokomak fusion reactors (principally the International Thermonuclear Experimental Reactor, ITER). Data published as early as 1979 [82] indicated that fibers with nominally pure-silica cores are most likely the materials of choice for such applications, and recent workers seem to concur.

A paper by Sylvain Girard and coworkers appearing in these proceedings [83] reports studies of pulsed-X-ray-induced optical absorption in two nominally pure-silica-core fibers at room temperature. These authors find that the 660 and 760 nm bands were induced by pulsed X rays (total dose ∼2 Gy, dose rate >1 MGy/s) in a low-OH/low-Cl silica-core fiber but not in a companion fiber with a high-OH silica core. Their decay data for the dominant 760 nm band, as well as their fractal-kinetic fits of these data, in the range 0.1–600 s are in harmony with my own isothermal decay data for similar fibers measured at the same wavelength, and my fractal-kinetic fits of these, in the range 60–8000 s following γ irradiation (dose 8.4×10^4 Gy, dose rate 1 Gy/s) [63]. But Sylvain's new data are the first I have seen since those published by Kaya Nagasawa [31,32] that show the 760 nm band to be more intense than its companion at 660 nm. The common element here would seem to be the low doses employed in these very different experiments (∼20–300 Gy in [31,32] versus ∼2 Gy in [83]) and certainly not the dose *rates* (0.02–0.07 Gy/s [31,32] versus >1 MGy/s [83]). We therefore have a strong hint that the relative peak absorptions of the 660 and 760 nm bands in comparable low-OH/low-Cl fibers may be *independent of dose rate* even at room temperature.

6.6. Theoretical calculations are dearly needed – and they are coming soon!

Additional high-quality quantum-chemical calculations of hole self-trapping in a-SiO_2 are dearly needed to continue to test the STH models I have put forward in [17]. Happily, such studies have already been initiated by René Corrales at Pacific Northwest National Laboratory and his student Margaret Gabriel at the University of Washington [84], as well as by Alex Shluger and Peter Sushko at University College London. Both studies involve placing holes in model glass 'samples' comprising 70 or more atoms in random networks selected for having both the correct mass density and diffraction patterns measured for real silica glasses. Both of these investigations are only months away from publication.

Using plane wave density functional theory with the PBE0 functional that is self-interaction corrected, René and Margaret found a family of STHs ranging from those with most spin density located on a single oxygen atom (generally matching STH_1 as illustrated in Fig. 4(e)) to extreme case where most spin density is shared between two adjacent oxygens (generally matching STH_2 as illustrated in Fig. 4(f)). However, in neither of these cases is the calculated spin density 100% on just one or two oxygens; rather, in all cases there is a residual spin density found to be distributed amongst a number of other oxygen neighbors. Finally, they found a third family member with the majority of the spin density spread over three oxygens, albeit unequally.

6.7. How and why to calculate STHs in a-SiO_2

As often stressed by Adrian Wright (e.g., [85–87]), neutron and X-ray diffraction studies place strong constraints on the possible structure(s) of silica glasses. Thus, any model glass that fails to replicate the diffraction patterns and mass density of a real glass is virtually worthless as a substrate for modeling of defect centers in real glasses. Adrian discusses structural order in vitreous silica in terms of four scale ranges [85–87]: I, the structural unit (SiO_4 tetrahedron); II, the interconnection of adjacent structural units; III, the network topology (including ring statistics); and IV, longer-range density fluctuations. Range-II order involves three variable parameters: the Si–O–Si bond angle and two torsional (dihedral) angles.

The STH_2 model of Fig. 4(f) places very strong constraints on the dihedral angles of the two bridging oxygens that share the trapped hole (consequent to the requirement that the two non-bonding O 2p orbitals in the *x–y* plane be the highest-energy occupied molecular orbitals in a-SiO_2). Surprisingly, it turns out that these same special dihedral angles actually occur for two of the four (range-II) interconnections *of each tetrahedron* in α quartz! But, as mentioned in Section 1, no self-trapped holes have been detected by ESR in α quartz despite a concerted effort [10]. Hayes and Jenkin [10] were forced to conclude that *long-range* hole hopping in quartz is much more rapid than the Larmour precession rate in the ESR experiment, even near 4 K. However, one can easily imagine an $[Al]^0$ analog of STH_2 in α quartz, where the hole would be coulombically pinned to the Al-substituted site and thus would be easily observable by ESR. Does this occur? According to the best available evidence ca. 1978 (see my review [74]), the ground-state hole of the $[Al]^0$ center is indeed localized on the very oxygens possessing the peculiar dihedral angles that I impute to STH_2 [88] and the hole in fact hops back and forth between these two degenerate ground-state oxygens on each AlO_4 tetrahedron [89]. However, this hopping between these two sites is not rapid enough to result in an STH_2-type spectrum. The observed $[Al]^0$ defect is thus modeled the same as STH_1 (Fig. 4(e)). Hence, if my STH_2 model of Fig. 4(f) continues to be validated, there must be polaronic relaxations and/or pre-existing distortions in a-SiO_2 that are of a different nature or magnitude than those in α quartz. Given that the crystal structure of α quartz is well known, the *g* tensor of a hypothetical 'STH_2-type' $[Al]^0$ center (forced by artificially introduced distortions) might be a target of further first-principles calculations of the type developed by Pickard and Mauri [44]. Among other things, such studies could fix the respective values of the parameter *M* in Eqs. (4b) and (5c).

6.8. Why should industry care?

The tumbling satellites of Section 4 are unlikely to be the last industrial problem to be resolved by understanding the fundamental natures of STHs in a-SiO_2. One reason for my confidence in this matter is that a-SiO_2 continues to play central roles in so many of today's technologies. It is still the most important material of fiber optics (including fibers exposed to nuclear or space radiations [90]); it is the gate and field insulator in 90% of contemporary MOSFETs (including computer chips) [91]; and it is used as windows, transmissive optics, and photomasks for ultraviolet (UV) microchip lithography that are vulnerable to damage by the very UV photons they are designed to guide. A second reason is that STHs are possibly the starting point of all irreversible radiation effects (including density changes, e.g., [59,60,92–95]) that occur in silica glasses. That is, if STHs should turn out to be *the first carriers to trap* in a-SiO_2, they would determine the sites of permanent damage to the network topology. This is because, by subsequently capturing free electrons, these STHs would then become self-trapped excitons (STEs) [96] – and the non-radiative decays of STEs are responsible for the formation of vacancy-interstitial pairs in most insulating materials [96,97]. Apropos, Tsung Tsai and I have shown unambiguously that non-radiative decays of STEs induced by multiphoton absorption of 6.4-eV excimer laser light lead to oxygen displacements in silica glass [98].

Finally, our improving ability to understand and control radiation-induced property changes in a-SiO_2 is already leading to new applications previously thought impossible.

Indeed, Hideo Hosono and coworkers (e.g., [26,99,100]) have begun to speak of certain 'modified silicas' as though they were 'new materials' for this very reason. An example is an optical fiber (for use, e.g., in medical applications or as tips for scanning near-field UV optical microscopy) that is immune to damage by the deep-UV photons that it guides [99]. At present, such fibers include some with low-OH/low-Cl, F-doped-silica cores (the same system that I selected to include in my studies of a decade ago [34–36]), as well as high-OH silicas that are 'hardened' against UV-photon-induced color-center formation by H_2 impregnation and pre-irradiation [26,99,100].

References

[1] W.B. Fowler (Ed.), Physics of Color Centers, Academic Press, New York, 1968.
[2] D.L. Griscom, in: D.R. Uhlmann, N.J. Kreidl (Eds.), Glass Science and Technology, Advances in Structural Analysis, vol. 4B, Academic Press, New York, 1990, p. 151.
[3] D.L. Griscom, in: O. El-Bayoumi, C.J. Simmons (Eds.), Experimental Techniques of Glass Science, The American Ceramic Society, Westerville, OH, 1993, p. 161.
[4] D. Emin, Adv. Phys. 22 (1973) 57.
[5] T.G. Castner, W. Känzig, J. Phys. Chem. Solids 3 (1957) 178.
[6] W.H. Zachariasen, J. Am. Chem. Soc. 54 (1932) 3841.
[7] P.W. Anderson, Phys. Rev. 109 (1958) 1492.
[8] N.F. Mott, Conduction in Non-Crystalline Materials, 2nd Ed., Clarendon, Oxford, 1993.
[9] N.F. Mott, Adv. Phys. 16 (1967) 49.
[10] W. Hayes, T.J.L. Jenkin, J. Phys. C 19 (1986) 6211.
[11] R.A. Weeks, J. Appl. Phys. 27 (1956) 1376.
[12] M. Stapelbroek, D.L. Griscom, E.J. Friebele, G.H. Sigel Jr., J. Non-Cryst. Solids 32 (1979) 313.
[13] D.L. Griscom, E.J. Friebele, Phys. Rev. B 24 (1981).
[14] E.J. Friebele, D.L. Griscom, M. Stapelbroek, R.A. Weeks, Phys. Rev. Lett. 42 (1979) 1346.
[15] A.V. Amosov, I.V. Wasserman, D.M. Yudin, in: Proc. 9th Int. Congr. Glass, Paris, 1971, Sect. A1.7, p. 107.
[16] D.L. Griscom, Phys. Rev. B 40 (1989) 4224.
[17] D.L. Griscom, J. Non-Cryst. Solids 149 (1992) 137.
[18] D.L. Griscom, J. Appl. Phys. 58 (1985) 2524.
[19] D.L. Griscom, D.B. Brown, N.S. Saks, in: C.R. Helms, B.E. Deal (Eds.), The Physics and Chemistry of SiO_2 and the Si–SiO_2 Interface, Plenum, New York, 1988, p. 287.
[20] D.L. Griscom, J. Electron. Mater. 21 (1992) 763.
[21] N.S. Saks, R.B. Klein, D.L. Griscom, IEEE Trans. Nuc. Sci. NS-35 (1988) 1234.
[22] N.S. Saks, R.B. Klein, S. Yoon, D.L. Griscom, J. Appl. Phys. 70 (1991) 7434.
[23] E.H. Poindexter, P.J. Caplan, Prog. Surf. Sci. 14 (1983) 201.
[24] D.L. Griscom, J. Non-Cryst. Solids 68 (1984) 301.
[25] T.E. Tsai, D.L. Griscom, E.J. Friebele, Phys. Rev. B 40 (1989) 6374.
[26] K. Kajihara, L. Skuja, M. Hirano, H. Hosono, Phys. Rev. Lett. 89 (2002) 135507.
[27] A.H. Edwards, J.A. Pickard, R.E. Stahlbush, J. Non-Cryst. Solids 179 (1994) 148.
[28] K.L. Brower, P.M. Lenahan, P.V. Dressendorfer, Appl. Phys. Lett. 41 (1982) 251.
[29] P.V. Chernov, E.M. Dianov, V.N. Karpechev, L.S. Kornienko, I.O. Morozova, A.O. Rybaltovskii, V.O. Sokolov, V.B. Sulimov, Phys. Status Solidi B 115 (1989) 663.
[30] E. Harari, S. Wang, B.S.H. Royce, J. Appl. Phys. 46 (1975) 1310.
[31] K. Nagasawa, M. Tanabe, K. Yahagi, Jpn. J. Appl. Phys. 23 (1984) 1608.
[32] K. Nagasawa, M. Tanabe, K. Yahagi, A. Iino, T. Kuroha, Jpn. J. Appl. Phys. 23 (1984) 606.
[33] D.L. Griscom, J. Non-Cryst. Solids 349 (2004) 139.
[34] D.L. Griscom, J. Appl. Phys. 80 (1996) 2142.
[35] D.L. Griscom, in: G.E. Matthews, R.W. Williams (Eds.), Defects in Insulating Materials ICDIM 96, Materials Sci. Forum 239–241 (1997) 19.
[36] D.L. Griscom, Appl. Phys. Lett. 71 (1997) 175.
[37] Y. Sasajima, K. Tanimura, Phys. Rev. B 68 (2003) 014204.
[38] R.A. Weeks, Phys. Rev. 130 (1963) 570.
[39] D.L. Griscom, Nucl. Instr. Methods B 1 (1984) 481.
[40] D.L. Griscom, Nucl. Instr. Methods B 46 (1990) 12.
[41] R.P. Wang, K. Saito, A.J. Ikushima, J. Non-Cryst. Solids 351 (2005) 1569.
[42] D.L. Griscom, in: G. Pacchioni, L. Skuja, D.L. Griscom (Eds.), Defects in SiO_2 and Related Dielectrics: Science and Technology, Kluwer, The Netherlands, 2000, p. 117.
[43] G. Pacchioni, A. Basile, Phys. Rev. B 60 (1999) 9990.
[44] C.J. Pickard, F. Mauri, Phys. Rev. Lett. 88 (2002) 086403.
[45] G.E. Peterson, C.R. Kurkjian, A. Carnavale, Phys. Chem. Glasses 15 (1974) 52.
[46] D.L. Griscom, in: Encyclopedia of Materials: Science and Technology, Elsevier, 2001, p. 179.
[47] P.H. Kasai, J. Chem. Phys. 43 (1965) 3322.
[48] J.A. Weil, Rad. Effects 26 (1975) 261.
[49] J.A. Weil, J.R. Bolton, J.E. Wertz, Electron Paramagnetic Resonance: Elemental Theory and Practical Applications, Wiley, New York, 1996.
[50] D.L. Griscom, J. Non-Cryst. Solids 31 (1978) 241.
[51] D.L. Griscom, E.J. Friebele, K.J. Long, J.W. Fleming, J. Appl. Phys. 54 (1983) 3743.
[52] D.L. Griscom, J. Non-Cryst. Solids 24 (1977) 155.
[53] S.T. Pantelides, W.A. Harrison, Phys. Rev. B 13 (1976) 2667.
[54] P.M. Schneider, W.B. Fowler, Phys. Rev. Lett. 36 (1976) 425.
[55] D. Emin, M.-N. Bussac, Phys. Rev. B 49 (1994) 14290.
[56] M. Yamaguchi, K. Saito, A.J. Ikushima, Phys. Rev. B 68 (2003) 153204.
[57] R.P. Wang, N. Tai, K. Saito, A.J. Ikushima, J. Appl. Phys. 98 (2005) 023701.
[58] K. Arai, H. Imai, J. Isoya, H. Hosono, Y. Abe, H. Imagawa, Phys. Rev. B 45 (1992) 10818.
[59] R.A.B. Devine, J. Arndt, Phys. Rev. B 35 (1987) 9376.
[60] R.A.B. Devine, J. Arndt, Phys. Rev. B 39 (1987) 5132.
[61] V.A. Bogatyrjov, I.I. Cheremisn, E.M. Dianov, K.M. Golant, A.L. Tomashuk, in: Proc. RADECS 95, Arcachon, France, 1995, p. 503.
[62] O. Deparis, D.L. Griscom, P. Mégret, M. Decréton, M. Blondel, J. Non-Cryst. Solids 216 (1997) 124.
[63] D.L. Griscom, Phys. Rev. B 64 (2001) 174201.
[64] S. Sen, R.L. Andrus, D.E. Baker, M.T. Murtagh, Phys. Rev. Lett. 93 (2004) 125902.
[65] D.-L. Kim, M. Tomozawa, S. Dubois, G. Orcel, J. Lightwave Technol. 19 (2001) 1155.
[66] E.J. Friebele, D.L. Griscom, M.J. Marrone, J. Non-Cryst. Solids 71 (1985) 133.
[67] D.L. Griscom, M. Mizuguchi, J. Non-Cryst. Solids 239 (1998) 66.
[68] Y. Hibino, H. Hanafusa, J. Appl. Phys. 60 (1986) 1797.
[69] Aviation Week & Space Technology, 7 December 1998, p. 24.
[70] M. McCants, <www.wingar.demon.co.uk/satevo/tle/iridstat.txt>.
[71] K. Nassau, B.E. Prescott, Phys. Stat. Solidi 29 (1975) 659.
[72] E.J. Friebele, in: D.R. Uhlmann, N.J. Kreidl (Eds.), Optical Properties of Glass, American Ceramic Society, Westerville, OH, 1991, p. 205.
[73] R. Schnadt, A. Räuber, Solid State Commun. 9 (1971) 159.
[74] D.L. Griscom, in: S.T. Pantelides (Ed.), The Physics of SiO_2 and Its Interfaces, Pergamon, New York, 1978, p. 232.
[75] NASA, 1999 Worldwide Space Launches. Available from: <www.hq.nasa.gov/osf/1999/launch99.html>.

[76] W.W. Chow, J. Gea-Banacloche, L.M. Pedrotti, V.E. Sanders, W. Schleich, M.O. Scully, Rev. Mod. Phys. 57 (1985) 61.
[77] D.L. Griscom, E.J. Friebele, Phys. Rev. B 34 (1986) 7524.
[78] L. Skuja, B. Güttler, Phys. Rev. Lett. 77 (1996) 2093.
[79] A. Edwards, W.B. Fowler, Phys. Rev. B 26 (1982) 6694.
[80] K. Kajihara, L. Skuja, H. Hirano, H. Hosono, Phys. Rev. Lett. 92 (2004) 015504.
[81] L. Skuja, K. Kajihara, T. Kinoshita, M. Hirano, H. Hosono, Nucl. Instr. Methods B 191 (2002) 127.
[82] E.J. Friebele, Opt. Eng. 18 (1979) 522.
[83] S. Girard, D.L. Griscom, J. Baggio, B. Brichard, F. Berghmans, these proceedings.
[84] M.A. Gabriel, PhD dissertation, Department of Chemistry, University of Washington, Seattle, WA, in preparation.
[85] A.C. Wright, J. Non-Cryst. Solids 106 (1988) 1.
[86] A.C. Wright, J. Non-Cryst. Solids 179 (1994) 84.
[87] A.C. Wright, in: G. Pacchioni, L. Skuja, D.L. Griscom (Eds.), Defects in SiO_2 and Related Dielectrics: Science and Technology, Kluwer, The Netherlands, 2000, p. 1.
[88] J.H. Mackey, J.W. Boss, D.E. Wood, J. Magn. Res. 3 (1970) 44.
[89] A.L. Taylor, G.W. Farnell, Canad. J. Phys. 42 (1964) 595.
[90] E.J. Friebele, M.E. Gingerich, D.L. Griscom, SPIE 1791 (1992) 177.
[91] A. Stesmans, J. Non-Cryst. Solids 179 (1994) 10.
[92] W. Primak, Phys. Rev. 110 (1958) 1240.
[93] J.A. Ruller, E.J. Friebele, J. Non-Cryst. Solids 136 (1991) 163.
[94] R.A.B. Devine, Nucl. Instt. Methods B 91 (1994) 378.
[95] C.K. Van Peski, R. Morton, Z. Bor, J. Non-Cryst. Solids 265 (2000) 285.
[96] K.S. Song, R.T. Williams, Self-Trapped Excitons, Springer, Heidelberg, 1993.
[97] N. Itoh, M. Stoneham, Materials Modification by Electronic Excitation, Cambridge University, 2001, 536pp.
[98] T.-E. Tsai, D.L. Griscom, Phys. Rev. Lett. 67 (1991) 2517.
[99] H. Hosono, M. Mizuguchi, H. Kawazoe, T. Ogawa, Appl. Phys. Lett. 74 (1999) 2755.
[100] M. Oto, S. Kikugawa, N. Sarukura, M. Hirano, H. Hosono, IEEE Photonics Tech. Lett. 13 (2001) 978.